ENHANCED SUPPORT VECTOR REGRESSION FOR IMPROVING ACCURACY IN PREDICTING SHEAR STRENGTH IN FIBER-REINFORCED POLYMER-REINFORCED CONCRETE BEAMS WITH FRP STIRRUPS

Thi Thu Ha Truong[1], Minh-Thao Le[2], Ngoc-Tri Ngo[2]*, Anh Duc Mai[2]

[1]The University of Danang - University of Technology and Education, Vietnam
[2]The University of Danang - University of Science and Technology, Vietnam

*Corresponding author: trinn@dut.udn.vn

(Received: March 29, 2026; Revised: May 15, 2026; Accepted: June 05, 2026)

DOI: 10.31130/ud-jst.2026.24(7B).580E

Abstract - Fiber-reinforced polymer (FRP)-reinforced concrete beams have increasingly applied in construction. Accurate prediction of shear strength in FRP-reinforced concrete beams with FRP stirrups is essential for safe and efficient structural design. This study aims to improve prediction accuracy by developing an enhanced support vector regression (SVR) model with the aid of an optimization algorithm, and a reliable dataset was evaluated using a 10-fold cross-validation approach. The proposed model achieved strong predictive capability with low error values. The enhanced SVR model with 200 wolves and 100 iterations provides the best performance, with RMSE, MAE, and MAPE values of 28.14kN, 19.27kN, and 15.40%, respectively, along with a correlation coefficient of 0.955. Furthermore, the optimized models outperformed conventional SVR models with different kernel functions. These findings indicate that the enhanced SVR approach is a reliable and effective tool for predicting shear strength, thereby supporting improved structural analysis and design in engineering practice.

Key words - Fiber-reinforced polymer; support vector regression; shear strength; FRP-reinforced concrete beams; optimization

1. Introduction

Fiber-reinforced polymer (FRP) bars have increasingly been utilized in concrete members as an alternative to conventional steel reinforcement to mitigate corrosion-induced deterioration [1]. Beyond their superior durability in corrosive environments, FRP bars exhibit lower self-weight, high tensile capacity, and non-magnetic behavior when compared with traditional steel reinforcement [2, 3]. Nevertheless, concrete beams reinforced with FRP tend to be more prone to shear failure than those reinforced with steel reinforcement [4]. The shear capacity of FRP-reinforced concrete (FRP-RC) beams is influenced by both concrete mechanical properties and the contribution provided by transverse FRP stirrups [1]. Therefore, a thorough understanding of shear strength mechanism is essential at the preliminary design stage of reinforced concrete structures.

Empirical equations and design codes, such as CSA S8-06, CSA S6-09, and ACI 440.11-22 have been commonly employed to estimate the shear capacity of concrete beams [5, 6]. For example, Di et al. [5] evaluated a comprehensive database of FRP-RC beams subjected to shear failure using several existing design codes. Results indicated that CSA S806–12 exhibited the most accurate predictions. However, these empirical methods and existing codes do not sufficiently account for the influences of varying failure mechanisms and the ultimate strain distribution in the stirrups when estimating the shear strength of FRP-reinforced beams. Most of these methods adopt conservative assumptions, which tend to underestimate the contribution of FRP stirrups and, consequently, the total shear capacity of the beam. Accordingly, the application of such design approaches in engineering practice may result in the use of an excessive amount of FRP stirrups, leading to increased construction costs and additional labor requirements [2].

Although traditional empirical methods have been widely employed to estimate the shear capacity of FRP-RC beams, their notable limitations in capturing complex and nonlinear behaviors of various parameters (e.g., concrete strength, effective depth, shear span-to-depth ratio, FRP material properties, reinforcement ratio, transverse stirrups) [6]. In the past years, the development of artificial intelligence (AI) has enabled researchers to address such nonlinearities more effectively in civil engineering. AI models like artificial neural networks (ANNs), random forest (RF), support vector regression (SVR) have demonstrated superior predictive performance compared with traditional empirical equations and existing design codes in predicting the shear strength of FRP-reinforced structural members [1, 7-9]. For instance, Alam et al. [8] adopted a generalized regression neural network for predicting the shear strength of FRP-RC members without transverse reinforcement. Analytical results showed that the proposed model exhibited higher prediction accuracy than existing design codes and guidelines, including ACI 440.1R, CSA S806, JSCE, and BISE.

Jumaa and Yousif [7] employed ANNs, gene expression programming (GEP), and nonlinear regression analysis (NLR) to predict the shear strength of FRP-RC elements without stirrups. Results indicated that both ANNs and the GEP models provided higher predictive accuracy and computational efficiency compared with available codes and formulas. Similarly, Ebid and Deifalla [10] developed a novel equation using the genetic programming technique to predict the capacity of FRP reinforced beam with and without stirrups. Findings revealed that the proposed method yielded more reliable and accurate predictions than those obtained from conventional design codes reported in the literature. In the study conducted by Yaseen [1], three ML models, including M5-Tree, extreme learning machine (ELM), and RF, were used for investigating the shear strength prediction capability of FRP-RC beams incorporating transverse reinforcement. Results indicated that the M5-Tree with nine inputs exhibited the highest predictive accuracy, followed by the ELM and RF models.

Although AI models achieve higher prediction accuracy than conventional empirical equations and design codes, the effectiveness of these standalone learners remains heavily dependent on the appropriate selection of their hyperparameters. Failing to optimize these parameters can significantly compromise model stability and generalization capability. Among AI algorithms, SVR is one of the most widely used models [11]. Accordingly, this study proposes an SVR model optimized by a metaheuristic algorithm to enhance the precision of shear strength predictions for FRP-reinforced concrete beams with stirrups. The performance of the proposed hybrid SVR model is compared with that of various single AI techniques. By leveraging advanced AI methodologies, this study offers structural designers a promising tool for addressing practical design challenges associated with FRP-reinforced concrete members.

2. Research methodology

2.1. Enhanced SVR and standalone SVR models

Regression difficulties are addressed by the supervised learning model known as the SVR model [12]. The non-linear relationship between the predictors and dependent variables can be effectively captured by the SVR. An SVR model is trained using a least-squares cost function to produce linear equations in a dual space that speeds up computation. In particular, solving Eq. (1) is used to teach SVR models.

$$\min_{\omega,b,e} J(\omega,b,e)=\frac{1}{2}\|\omega\|^2+\frac{1}{2}C\sum_{k=1}^{n}e_k^2;$$

$$\text{subject to } y_k=\langle\omega,\varphi(x_k)\rangle+b+e_k,\ k=1,\ldots n \quad (1)$$

where $J(\omega,b,e)$ is an objective function; ω is a linear approximator`s parameter; e_k is errors; $C\geq 0$is a regularization parameter; x_k is predictors; y_k is dependent; b is bias; and n is the dataset size.

This problem is solved by using Lagrange multipliers (α_k), which leads to Eq. (2). Equation (3) describes a kernel function. The Gaussian radial basis functions (RBF) kernel is a potent kernel function that is used in this work and is shown in Eq. (4).

$$f(x)=\sum_{k=1}^{n}\alpha_k K(x,x_k)+b \quad (2)$$

$$K(x,x_k)=\sum_{k=1}^{n}g_k(x)g_k(x_k) \quad (3)$$

$$K(x,x_k)=exp(-\|x-x_k\|^2/2\sigma^2) \quad (4)$$

where are α_k is Lagrange multipliers; $K(x,x_k)$ is the kernel function; σ is the RBF width.

The enhanced SVR model in this study was proposed by integrating with a meta-heuristic namely grey wolf optimizer (GWO). Introduced by Mirjalili et al. [13], the GWO algorithm draws inspiration from the natural social hierarchy and predatory behaviors of grey wolves. The GWO optimized the standalone SVR's hyperparameters, including RBF width *(σ)* and the regularization parameter (C).

Two standalone SVR models was also used in this study, including SVR with the Pearson VII function-based universal kernel.SVR (SVR_Puk) and SVR with the polynomial kernel (SVR_Poly).

2.2. Dataset

To assess the predictive performance of the proposed optimized SVR model, a real-world dataset was prepared, which was collected from previous work. The dataset involved 161 samples of FRP-reinforced concrete beams with FRP stirrups [14-46]. Outliers were removed before training and testing the proposed model, resulting 135 samples in the dataset. Aramid fiber-reinforced polymer (AFRP), Basalt fiber-reinforced polymer (BFRP), Carbon fiber-reinforced polymer (CFRP), and Glass fiber-reinforced polymer (GFRP) were used as longitudinal reinforcement and stirrups in the dataset. Table 1 details data attributes of FRP-reinforced concrete beams with FRP stirrups in this study. It describes the range values of data attributes, which include the information for the specimen size attributes, the compressive concrete strength, the longitudinal reinforcement attributes, the stirrups attributes, and the ultimate shear capacity of beams. Figure 1 visualizes histograms for data attributes.

Table 1. *Data attributes of FRP-RC beams with FRP stirrups*

Attribute groups	Variables	Unit	[Min – max]	Average
Specimen size	Web width (b)	mm	120 - 300	182.61
	Effective depth (d)	mm	170 - 412	252.65
	Shear span ratio (a/d)	n/a	1.11 - 4.49	2.55
Concrete	Compressive concrete strength (f'_c)	MPa	19.60 - 73.40	38.33
Longitudinal reinforcement	Type of longitudinal reinforcement	n/a	GFRP, BFRP, AFRP, CFRP	
	Longitudinal reinforcement ratio (ρ_{fl})	%	0.39 - 3.98	1.63
	Elastic modules of FRP longitudinal reinforcements (E_{fl})	GPa	29.00 - 105.00	57.04
	Ultimate tensile strength of shear reinforcement from coupon tests (f_{ful})	MPa	480.00 - 1308.00	1016.00
Stirrups	Type of stirrups	n/a	GFRP, BFRP, CFRP, AFRP	
	Shear reinforcement ratio (ρ_{fv})	%	0.11 - 1.50	0.55
	Elastic modules of FRP shear reinforcements (E_{fv})	GPa	26.50 - 115.00	53.16
	Effective stress of shear reinforcement at failure (f_{fuv})	MPa	524.00 - 1700.00	964.01
Predictor	Ultimate shear capacity of beams (V_{exp})	kN	20.45 - 459.00	138.61

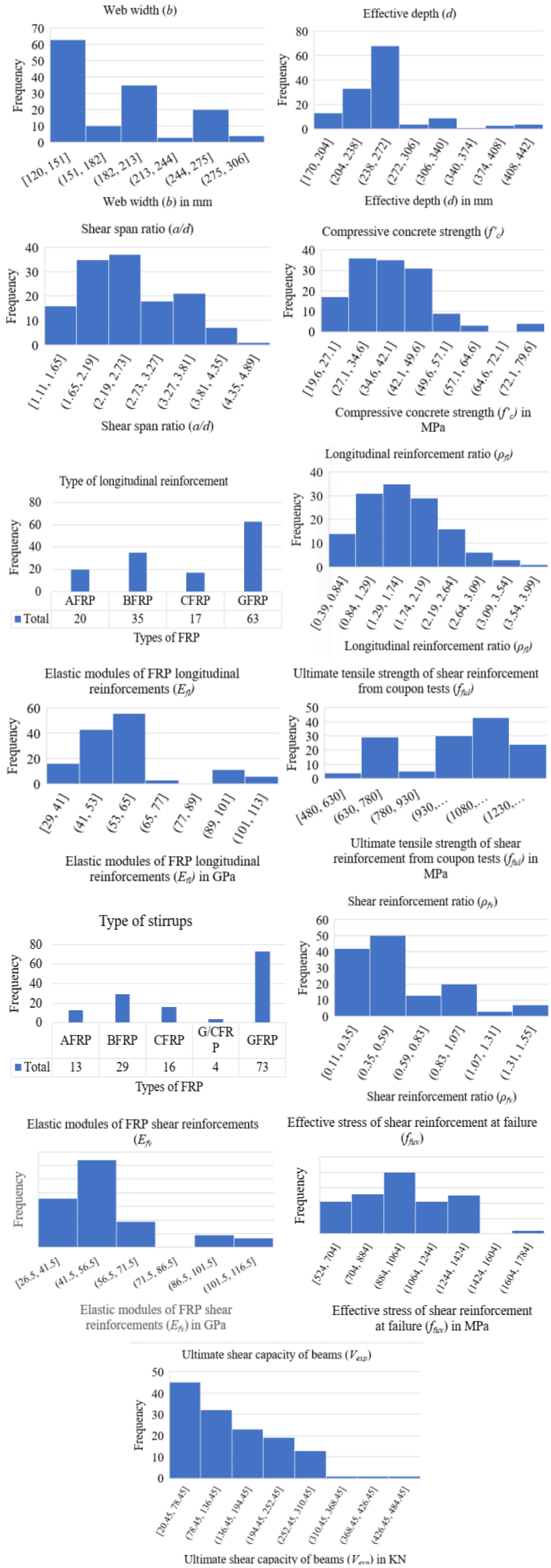

Figure 1. *Histograms for data attributes of FRP-RC beams with FRP stirrups*

3. Evaluation results

The proposed model was trained and tested using the mentioned dataset of FRP-RC beams with FRP stirrups. In this study, a 10-fold cross-validation was utilized to separate the dataset to the training part and the test part for evaluation purposes. Figure 2 visualizes the process of random generation for ten folds. Statistical measures were used to evaluate the performance of the model, which consists of correlation coefficient (R), root mean square error (RMSE), mean absolute error (MAE), and mean absolute percentage error (MAPE).

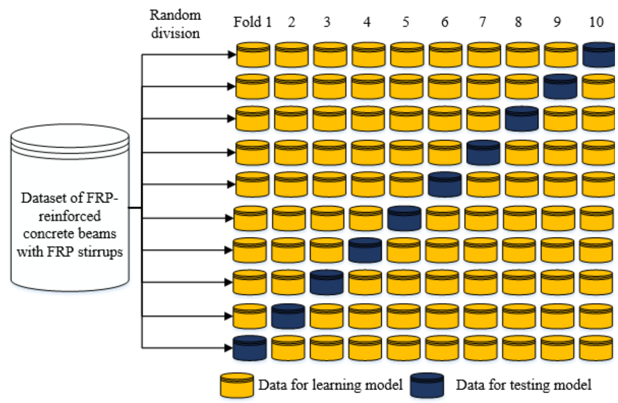

Figure 2. *A process of 10-fold cross-validation approach*

Table 2 presents settings of the optimized SVR model and evaluation scenarios to optimize and evaluate the SVR model. The 10-fold cross-validation method was applied. Two scenarios with different settings of GWO algorithms were used. The first scenario was set with 100 grey wolves and 50 iterations, while the second scenario was set with 200 grey wolves and 100 iterations.

Table. 2. *Parameters for the optimized SVR model*

Model	Parameter	Value
SVR model	Regularization parameter C	0.001 - 1000
	RBF width σ	0.001 - 1000
	Kernel function	Radial basis function
Grey wolf optimizer with the scenario 1	Number of grey wolves	100
	Maximum iteration	50
Grey wolf optimizer with the scenario 2	Number of grey wolves	200
	Maximum iteration	100

Table 3 presents the evaluation results of the optimized SVR model with the scenario 1 (100 grey wolves and 50 iterations) for inferring the shear strength of FRP-RC beams with FRP stirrups. Overall, the model demonstrated satisfactory generalization capability, with average RMSE values of 24.49 kN for the training data and 29.99 kN for the test data. Similarly, the MAE showed a moderate increase in prediction error when moving from training to testing data, with the average MAE_Tr and MAE_Te being 15.90 kN and 21.46 kN, respectively. The correlation coefficient confirmed strong predictive performance and the robustness of the model, with values of 0.959 (R_Tr) and 0.942 (R_Te).

Table 3. *Prediction accuracy of enhanced SVR model with scenario 1 (number of grey wolves = 100 and iteration = 50*

Fold	Evaluation indices							
	RMSE_Tr (kN)	RMSE_Te (kN)	MAE_Tr (kN)	MAE_Te (kN)	R_Tr (kN)	R_Te (kN)	MAPE_Tr(%)	MAPE_Te(%)
Fold1	27.97	17.81	17.97	15.12	0.950	0.974	15.18	**11.47**
Fold 2	21.26	56.86	14.92	35.71	0.967	0.891	12.80	26.98
Fold 3	17.85	58.71	11.79	38.09	0.977	0.867	10.90	20.21
Fold 4	23.54	29.77	15.28	20.90	0.963	0.949	12.85	20.89
Fold 5	24.75	22.96	15.78	17.81	0.960	0.940	13.26	12.62
Fold 6	28.29	39.22	18.06	28.72	0.945	0.937	15.50	25.14
Fold 7	27.98	**15.45**	18.11	**12.99**	0.949	**0.978**	14.87	16.26
Fold 8	27.34	16.62	17.42	13.40	0.951	0.969	14.11	14.16
Fold 9	27.39	19.45	17.56	14.38	0.951	0.972	14.55	11.80
Fold 10	18.53	23.04	12.12	17.50	0.978	0.940	10.52	13.98
Ave.	**24.49**	**29.99**	**15.90**	**21.46**	**0.959**	**0.942**	**13.45**	**17.35**
Min.	17.85	15.45	11.79	12.99	0.945	0.867	10.52	11.47
Max.	28.29	58.71	18.11	38.09	0.978	0.978	15.50	26.98
Std.	4.03	16.26	2.39	9.36	0.012	0.037	1.72	5.62

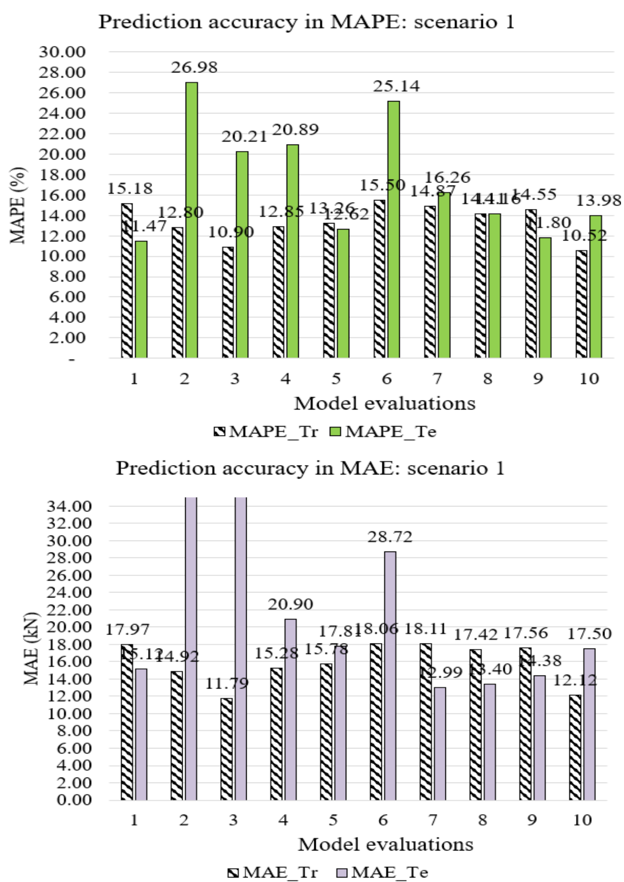

Figure 3. *Prediction accuarcy via MAPE and MAE for scenario 1*

In addition, the average MAPE values of 13.45% for training and 17.35% for testing suggested acceptable relative error levels for engineering applications. Notably, Fold 7 exhibited superior performance, with the lowest RMSE_Te and MAE_Te, and the highest R_Te, reflecting the variability in data distribution among the folds. The standard deviation values further indicated that, although the model was generally stable, some dispersion in testing performance still existed, particularly for RMSE_Te and MAPE_Te.

To further illustrate the model performance, Figure 3 presents the variation of MAPE and MAE across the 10 folds for scenario 1. Consistent with the results in Table 3, the testing errors (MAPE_Te and MAE_Te) were generally higher than the training errors, with some folds (e.g., Fold 2 and Fold 6) showing relatively larger deviations due to data variability. In addition, Figure 4 demonstrated that the predicted values closely follow the actual shear strength in both training and testing phases, thereby confirming the reliability and generalization capability of the proposed model.

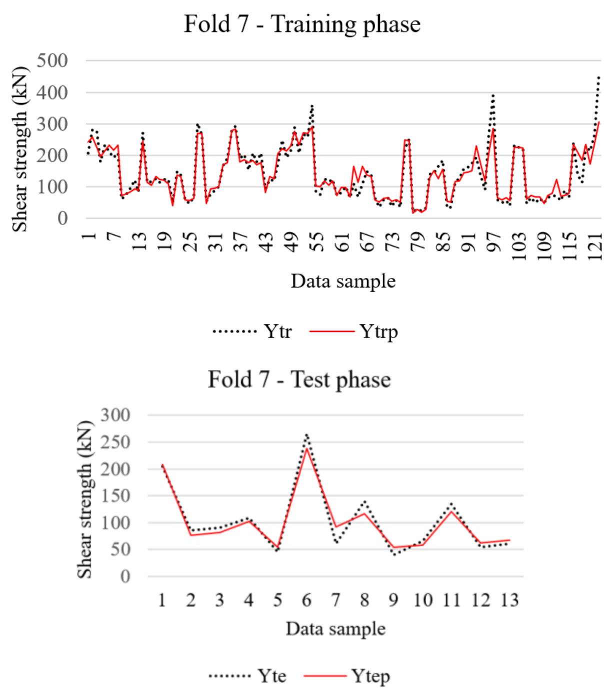

Figure 4. *Plot of actual and predicted values of shear strength for fold 7 – scenario 1*

Table 4 presents the predictive performance of the optimized SVR model under scenario 2 (200 grey wolves and 100 iterations) based on a 10-fold cross-validation scheme. Overall, the model demonstrated improved prediction accuracy compared to scenario 1 across all evaluation metrics. The average RMSE values were 23.54 kN for the training set and 28.14 kN for the test set. Notably, Fold 3 exhibited the lowest prediction errors in the testing phase across all performance measures, with MAE and MAPE values of only 8.97 kN and 7.61%, respectively. The correlation coefficient remained high and showed slight improvement, with average values of 0.962 for training and 0.955 for testing, confirming the robustness of the model. In terms of relative error, the average MAPE values decreased to 12.90% (training) and 15.40% (testing), further demonstrating the enhanced performance of scenario 2. Moreover, the standard deviation values indicated that although some variability in testing performance persisted, it was generally lower than that observed in scenario 1.

Table 4. *Prediction accuracy of optimized SVR model with scenario 2 (number of grey wolves = 200 and iteration = 100)*

Fold	Evaluation indices							
	RMSE_Tr (kN)	RMSE_Te (kN)	MAE_Tr (kN)	MAE_Te (kN)	R_Tr (kN)	R_Te (kN)	MAPE_Tr (%)	MAPE_Te (%)
Fold 1	26.94	29.12	17.47	21.98	0.953	0.928	14.66	20.41
Fold 2	26.64	24.07	17.14	17.65	0.954	0.943	14.37	14.31
Fold 3	27.97	**11.28**	18.26	**8.97**	0.950	**0.987**	15.22	**7.61**
Fold 4	26.36	42.66	16.65	23.17	0.951	0.946	14.06	12.75
Fold 5	23.19	27.55	14.73	18.85	0.964	0.965	12.06	13.64
Fold 6	20.22	54.85	14.07	34.24	0.969	0.912	12.22	21.69
Fold 7	26.91	20.00	17.34	14.62	0.954	0.966	14.45	11.90
Fold 8	14.73	35.39	9.58	27.19	0.985	0.952	8.50	28.75
Fold 9	16.34	17.47	10.89	13.22	0.983	0.968	9.53	12.27
Fold 10	26.10	19.04	16.88	12.85	0.955	0.982	13.96	10.61
Average	**23.54**	**28.14**	**15.30**	**19.27**	**0.962**	**0.955**	**12.90**	**15.40**
Min.	14.73	11.28	9.58	8.97	0.950	0.912	8.50	7.61
Max.	27.97	54.85	18.26	34.24	0.985	0.987	15.22	28.75
Std.	4.80	13.09	2.97	7.58	0.013	0.023	2.29	6.32

Figure 5 illustrates the performance of MAPE and MAE across 10 folds for scenario 2. It can be seen that lower errors were achieved compared to scenario 1, despite some fluctuations in fold 6 and fold 8. This pattern is consistent with the reduced average error metrics and highlights the enhanced predictive stability of the model. Furthermore, Figure 6 demonstrates a strong agreement between actual and predicted shear strength values in both training and test data, thereby confirming the reliability and generalization capability of the optimized SVR model under scenario 2.

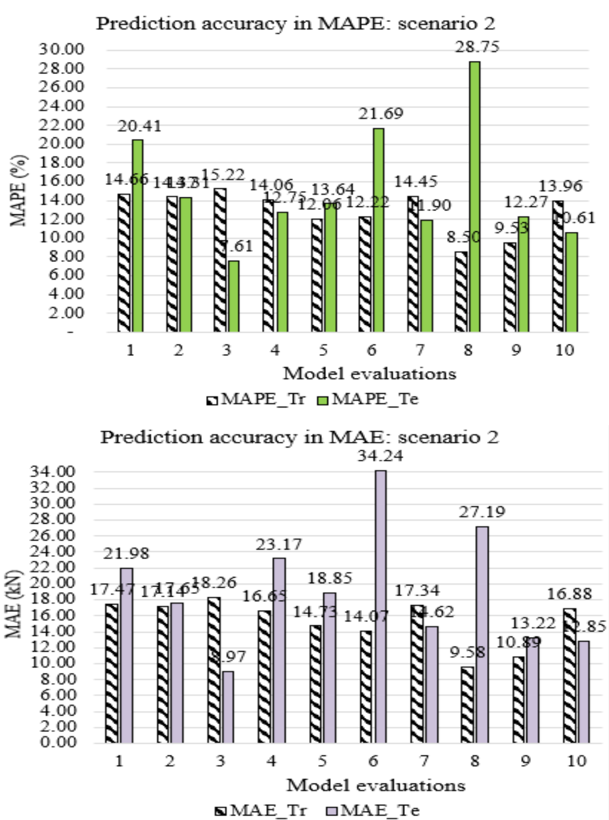

Figure 5. *Prediction accuracy via MAPE and MAE for scenario 2*

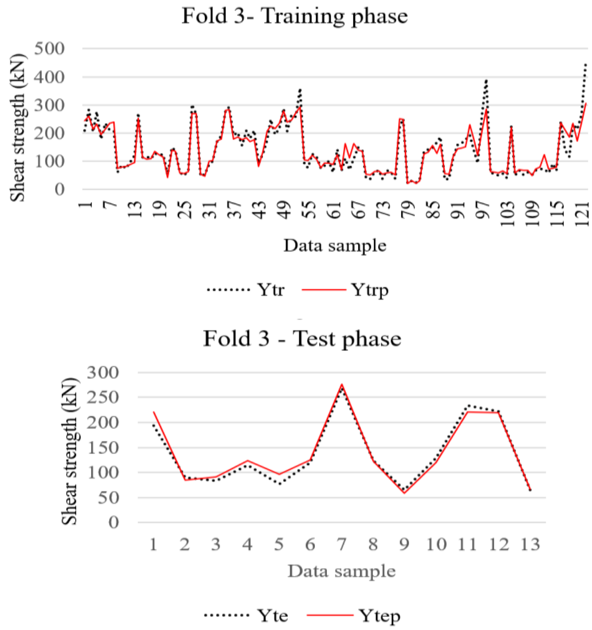

Figure 6. *Plot of actual and predicted values of shear strength for fold 3 – scenario 2*

Table 5 compares the predictive performance of two optimized SVR models with three standalone SVR models using different kernel functions. The results indicated that both optimized SVR models outperformed the conventional SVR approaches across all evaluation metrics. In particular, the optimized SVR under scenario 2 achieved the lowest prediction errors, with MAE and MAPE values of 19.27 kN and 15.40%, respectively, along with a higher correlation coefficient (R = 0.955).

Table 5. *Prediction accuracy of optimized SVR models and standalone SVR models*

Model	RMSE_Te (kN)	MAE_Te (kN)	R_Te	MAPE_Te (%)
Optimized SVR with scenario 1	29.99	21.46	0.942	17.35
Optimized SVR with scenario 2	**28.14**	**19.27**	**0.955**	**15.40**
SVR_RBF	47.83	31.02	0.865	24.38
SVR_Puk	38.96	21.35	0.892	16.62
SVR_Poly	37.50	24.73	0.899	26.65

Note: SVR_RBF is SVR with RBF function, SVR_Puk is SVR with the Pearson VII function-based universal kernel.SVR_Poly is SVR with the polynomial kernel.

In contrast, the standalone models, especially SVR_RBF, exhibited significantly higher prediction errors and lower correlation coefficients, indicating limited generalization capability. Although SVR_Puk and SVR_Poly showed relatively better performance among the baseline models, they still fell short compared to the optimized approaches. Figure 7 plot of actual and predicted values of shear strength by SVR_Puk, SVR_Poly, and SVR_RBF models. These findings confirm that the integration of GWO significantly enhanced the prediction accuracy and robustness of the SVR model, particularly under the more intensive optimization configuration of scenario 2.

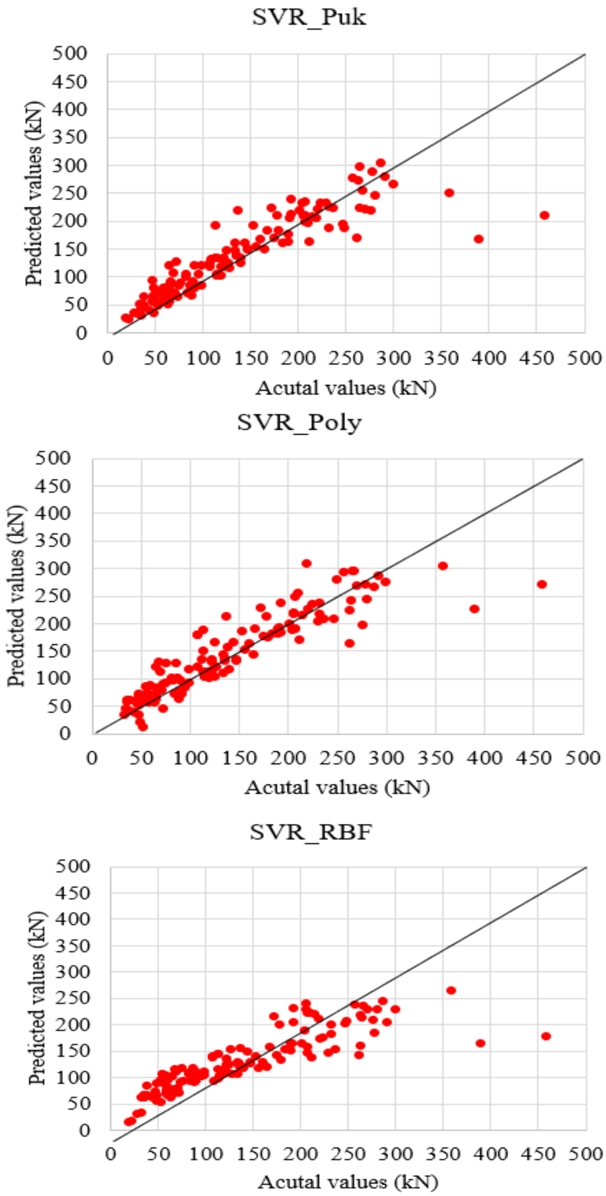

Figure 7. *Plot of actual and predicted values of shear strength by SVR_Puk, SVR_Poly and SVR_RBF models*

4. Conclusions

This study proposed an optimized SVR model integrated with the GWO to improve the prediction accuracy of shear strength in FRP-RC beams with transverse FRP stirrups. The results demonstrate that the proposed approach achieves high predictive performance, characterized by strong correlation coefficients and low error metrics across the cross-validation process. Among the two optimization configurations, the second scenario, which adopts 200 wolves and 100 iterations consistently yields superior accuracy, highlighting the effectiveness of a more intensive optimization strategy.

Compared with conventional SVR models employing different kernel functions, the optimized SVR approach exhibits clear improvements in both accuracy and stability. This enhancement underscores the capability of the GWO algorithm to effectively identify optimal hyperparameters and to better capture the complex nonlinear relationships inherent in the data. Overall, the proposed GWO–SVR model provides a robust and reliable tool for practical engineering applications. To facilitate real-world implementation, the developed GWO-SVR framework can be integrated into a standalone spreadsheet tool or a user-friendly Graphical User Interface. By simply inputting standard geometric and material design parameters, practicing engineers can instantaneously obtain exact estimations of the ultimate shear capacity without the need for time-consuming finite element modeling or cost-intensive experimental testing. Therefore, the proposed model serves as a rapid decision-support system during the early design phase, enabling the optimization of FRP reinforcement layouts and the efficient validation of structural safety margins in construction practice.

Future research should investigate the effect of input variables on the shear strength and rank these influential factors. Furthermore, the study needs focusing on expanding the dataset, incorporating additional influencing parameters, and exploring hybrid or alternative optimization techniques to further improve model performance and generalizability. The influence of varying fiber types and reinforcement arrangements on model performance should be investigated in future studies.

Acknowledgments: This research is funded by Vietnam Ministry of Education and Training under the project code B2024.DNA.02

REFERENCES

[1] Z. M. Yaseen, "Machine learning models development for shear strength prediction of reinforced concrete beam: a comparative study," *Scientific Reports,* vol. 13, p. 1723, 2023.

[2] X. Xue, L. Lin, J. Gao, and L. Chen, "Enhancing shear strength predictions for FRP-Reinforced concrete beams: Focusing on reasonable assessment of average ultimate strain in stirrups," *Structures,* vol. 71, p. 107900, 2025.

[3] X. Liang, J. Peng, and R. Ren, "A state-of-the-art review: Shear performance of the concrete beams reinforced with FRP bars," *Construction and Building Materials,* vol. 364, p. 129996, 2023.

[4] H. P. Nam *et al.*, "Development of shear strength prediction model for RC beams strengthened with FRP strips based on a novel ensemble learning model," *The University of Danang - Journal of Science and Technology,* vol. 22, no. 6A, pp. 13-18, 2024. doi:10.31130/ud-jst.2024.628E

[5] B. Di, Y. Zheng, J. Liao, J.-T. Fang, J.-J. Zeng, and Y. Zhuge, "Ultimate shear capacity of FRP-reinforced concrete beams: Test database and an improved design model," *Structures,* vol. 80, p. 109677, 2025.

[6] N. H. Dinh, Y.-S. Roh, and G. T. Truong, "Shear strength model of FRP-reinforced concrete beams without shear reinforcement," *Structures,* vol. 64, p. 106520, 2024.

[7] G. B. Jumaa and A. R. Yousif, "Predicting Shear Capacity of FRP-Reinforced Concrete Beams without Stirrups by Artificial Neural Networks, Gene Expression Programming, and Regression Analysis," *Advances in Civil Engineering,* vol. 25, 2018.

[8] M. S. Alam and U. Gazder, "Shear strength prediction of FRP reinforced concrete members using generalized regression neural network," *Neural Computing and Applications,* vol. 32, pp. 6151-6158, 2020/05/01 2020.

[9] M. A. Duc, "Application of machine learning models in predicting the compressive strength of GFRP-confined concrete," *The University of Danang - Journal of Science and Technology,* vol. 23, no. 6A, pp. 29-35, 2025. doi:10.31130/ud-jst.2025.23(6A).280.

[10] A. M. Ebid and A. Deifalla, "Prediction of shear strength of FRP reinforced beams with and without stirrups using (GP) technique," *Ain Shams Engineering Journal,* vol. 12, pp. 2493-2510, 2021.

[11] J. Zhang and Y. Wang, "Evaluating the bond strength of FRP-to-concrete composite joints using metaheuristic-optimized least-squares support vector regression," *Neural Computing and Applications,* vol. 33, pp. 3621-3635, 2021.

[12] J. A. K. Suykens, T. V. Gestel, J. D. Brabanter, B. D. Moor, and J. Vandewalle, *Least squares support vector machines*. Singapore: World Scientific, 2002.

[13] S. Mirjalili, S. M. Mirjalili, and A. Lewis, "Grey Wolf Optimizer," *Advances in Engineering Software,* vol. 69, pp. 46-61, 2014.

[14] T. Nagasaka, H. Fukuyama, and M. Tanigaki, "Shear Performance of Concrete Beams Reinforced With FRP Stirrups," in *SP-138: Fiber-Reinforced-Plastic Reinforcement for Concrete Structures - International Symposium*, 1993, pp. 789-812.

[15] K. Maruyama and W. J. Zhao, "Flexural and shear behaviour of concrete beams reinforced with FRP rods," *Corros Corros Prot Steel Concr* vol. 45, pp. 1330-1339, 1994.

[16] T. Okamoto, T. Nagasaka, and M. Tanigaki, "Shear capacity of concrete beams using FRP reinforcement," *Journal of Structural and Construction Engineering (Transactions of AIJ),* vol. 59, pp. 127-136, 1994.

[17] W. Zhao, K. Maruyama, H. Suzuki, and Rilem, "Shear behavior of concrete beams reinforced by FRP rods as longitudinal and shear reinforcement," in *2nd International symposium, Non-metallic (FRP) reinforcement for concrete structures*, Ghent; Belgium, 1995, pp. 352-359.

[18] P. V. Vijay, S. V. Kumar, and H. V. S. GangaRao, "Shear and ductility behavior of concrete beams reinforced with GFRP rebars," in *Proceedings of The 2nd International Conference on Advanced Composite Materials In Bridges and Structures, ACMBS-II*, Montreal, Canada, 1996, pp. 217-226.

[19] N. Duranovic, K. Pilakoutas, and P. Waldron, "Tests on concrete beams reinforced with glass fibre reinforced plastic bars," in *Proceedings of the Third International Symposium on Non-metallic (FRP) reinforcement for concrete structures (FRPRCS-3)*, Japan, 1997.

[20] T. Alkhrdaji, M. Wideman, A. Belarbi, and A. Nanni, "Shear Strength of GFRP RC Beams and Slabs," in *International Conference Composites in Constructions*, 2001, pp. 409-414.

[21] T. Imjai, "*Design and analysis of curved FRP composites as shear reinforcement for concrete structures,*" Department of Civil and Structural Engineering, University of Sheffield, 2008.

[22] J. Niewels, "Load carrying behaviour of concrete members with fibre reinforced polymers," RWTH Aachen, Germany, 2008.

[23] E. C. Bentz, L. Massam, and M. P. Collins, "Shear Strength of Large Concrete Members with FRP Reinforcement," *Journal of Composites for Construction,* vol. 14, pp. 637-646, 2010.

[24] D. Tomlinson and A. Fam, "Performance of Concrete Beams Reinforced with Basalt FRP for Flexure and Shear," *Journal of Composites for Construction,* vol. 19, p. 04014036, 2014.

[25] J. Hegger and M. Kurth, "Shear capacity of concrete beams with FRP reinforcement," in *SP-275: Fiber-Reinforced Polymer Reinforcement for Concrete Structures 10th International Symposium*, Florida, America, 2011, pp. 1–14.

[26] M. Said, M. Adam, A. Mahmoud, and A. Shanour, "Experimental and analytical shear evaluation of concrete beams reinforced with glass fiber reinforced polymers bars," *Construction and Building Materials,* vol. 102, pp. 574-591, 01/15 2016.

[27] G. B. Jumaa and A. R. Yousif, "Size effect on the shear failure of high-strength concrete beams reinforced with basalt FRP bars and stirrups," *Construction and Building Materials,* vol. 209, pp. 77-94, 2019.

[28] A. Al-Hamrani and W. Alnahhal, "Shear behavior of basalt FRC beams reinforced with basalt FRP bars and glass FRP stirrups: Experimental and analytical investigations," *Engineering Structures,* vol. 242, p. 112612, 2021.

[29] M. Krall and M. A. Polak, "Concrete beams with different arrangements of GFRP flexural and shear reinforcement," *Engineering Structures,* vol. 198, p. 109333, 2019.

[30] S. Tottori and H. Wakui, "Shear Capacity of RC and PC Beams Using FRP Reinforcement," in *SP-138: Fiber-Reinforced-Plastic Reinforcement for Concrete Structures - International Symposium*, 1993, pp. 615-632.

[31] H. Nakamura and T. Higai, " Evaluation of shear strength of concrete beams reinforced with FRP," *Doboku Gakkai Ronbunshu,* vol. 1995, pp. 89-100, 1995.

[32] M. Guadagnini, K. Pilakoutas, and P. Waldron, "Shear resistance of FRP RC beams: Experimental study," *Journal of Composites for Construction,* vol. 10, pp. 464-473, 2006.

[33] M. Issa, T. Ovitigala, and M. Ibrahim, "Shear Behavior of Basalt Fiber Reinforced Concrete Beams with and without Basalt FRP Stirrups," *Journal of Composites for Construction,* vol. 20, p. 04015083, 2015.

[34] L. Ascione, G. Mancusi, and S. Spadea, "Flexural Behaviour of Concrete Beams Reinforced With GFRP Bars," *Strain,* vol. 46, pp. 460-469, 2010.

[35] S. Spadea, "Comportamento di elementi di calcestruzzo armato con barre di materiale composito fibrorinforzato," *University Salerno,* vol. 4, pp. 60-69, 2010.

[36] S. W. Li, "*Experimental study on shear properties of BFRP-reinforced sea sand concrete beams*," Guangdong University of Technology, Guangzhou, China 2014.

[37] F. Yang, "*Deformation behaviour of beams reinforced with fibre reinforced polymer bars under bending and shear*," University of Sheffield, United Kingdom, 2015.

[38] D. J. Han, Z. X. Liu, and H. X. Liu, "Experimental study on the shear properties of recycled concrete beams enhanced by basalt fiber reinforcement," *FRP/Compos,* vol. 02, pp. 15-20, 2018.

[39] X. C. Fan and Z. R. Zhou, "Experimental study on shear properties of basalt reinforced inorganic polymer concrete beams," *Concrete,* vol. 06, pp. 100-104, 2019.

[40] S. H. Alsayed, "Flexural behaviour of concrete beams reinforced with GFRP bars," *Cement and Concrete Composites,* vol. 20, pp. 1-11, 1998.

[41] E. Shehata, R. Morphy, and S. Rizkalla, "Fibre reinforced polymer shear reinforcement for concrete members: Behaviour and design guidelines," *Canadian Journal of Civil Engineering,* vol. 27, pp. 859-872, 2011.

[42] T. Imjai, M. Guadagnini, and K. Pilakoutas, "Shear crack induced deformation of FRP RC beams," in *8th International Symposium on Fibre-Reinforced Polymer Reinforcement for Concrete Structures*, Patras, Greece, 2007.

[43] S. Cholostiakow, M. Di Benedetti, K. Pilakoutas, and M. Guadagnini, "Effect of beam depth on shear behavior of FRP RC beams," *Journal of Composites for Construction,* vol. 23, p. 04018075, 2018.

[44] A. Al-Hamrani, W. Alnahhal, and A. Elahtem, "Shear behavior of green concrete beams reinforced with basalt FRP bars and stirrups," *Composite Structures,* vol. 277, p. 114619, 2021.

[45] K. Chen, C. T. Zang, and L. Wang, "Experimental study on shear properties of carbon fiber composite reinforced concrete beams," *Building Science,* vol. 35, pp. 57-63, 2019.

[46] J. M. Lv, J. R. Pan, and B. Di, "Experimental study on the shear performance of self- compacting concrete beams with full GFRP reinforced seawater sea sand Research," *presented at the Concrete*, 2021.